Copyright © 1990 by the Genetics Society of America

Spatial Autocorrelation of Genotypes Under Directional Selection

B. K. Epperson

Department of Botany and Plant Sciences, University of California, Riverside, California 92521

Manuscript received July 3, 1989
Accepted for publication November 14, 1989

ABSTRACT

The spatial distributions of genetic variation under selection-mutation equilibrium within populations that have limited dispersal are investigated. The results show that directional selection with moderate strength rapidly reduces the amount of genetic structure and spatial autocorrelations far below that predicted for selectively neutral loci. For the latter, homozygotes are spatially clustered into separate areas or patches, each consisting of several hundred homozygotes. When selection is added the patches of the deleterious homozygotes are much smaller, in the range of 25 to 50 individuals. Selection also reduces temporal correlations. Also investigated are the effects of random replacement processes, such as mutation, immigration, and long-distance migration, on spatial and temporal correlations. The detection of natural selection through spatial pattern analysis is discussed, and applied to data from populations of the morning glory, *Ipomoea purpurea*.

NATURAL selection and gene dispersal control the spatial patterns of genetic variation within populations. However, there have been few theoretical results on precisely how selection changes spatial patterns of genetic variation. Theoretical studies have become increasingly important during the past decade since superior statistical methods for spatial pattern analysis were introduced to the field of population biology (SOKAL and ODEN 1978a, b). For genetic data, precise estimates of spatial autocorrelation statistics and other measures can be obtained from spatially arranged samples of moderate sizes from natural populations (see review in EPPERSON 1989). Most empirical studies have analyzed patterns of genetic variation *among* populations (*e.g.*, SOKAL and MENOZZI 1982; SOKAL, SMOUSE and NEEL 1986; SOKAL, ODEN and BARKER 1987; SOKAL and WINKLER 1987). The few studies of spatial patterns of genetic variation *within* populations, have demonstrated the power of spatial autocorrelation analyses for describing genetic structure, and for detecting natural selection (SOKAL and ODEN 1978b; EPPERSON and CLEGG 1986; DEWEY and HEYWOOD 1988; EPPERSON and ALLARD 1989; WAGNER *et al.* 1988; SCHOEN and LATTA 1989).

Predictable and striking spatial patterns are produced for selectively neutral loci in populations with limited symmetrical dispersal. Moran's measure of spatial correlation of allele frequencies as well as the coefficient of kinship (the probability that two randomly chosen genes are identical by descent) decrease exponentially with the physical distance separating locations (MALECOT 1948, 1973; BARBUJANI 1987). Marked patch structures quickly develop from local stochastic events and assortative matings. Homozygous genotypes become concentrated into separate large areas or patches, and these patches are surrounded by heterozygotes (TURNER, STEPHENS and ANDERSON 1982; SOKAL and WARTENBERG 1983; SOKAL, JACQUEZ and WOOTEN 1989).

The only detailed theoretical investigation into how different forms of natural selection change spatial distributions of genetic variation within populations was conducted by SOKAL, JACQUEZ and WOOTEN (1989). In these simulations the relative fitnesses of different genotypes depended on their location in different microenvironments within the population. Their results showed that microenvironmental selection can change spatial patterns of genetic variation, but the exact forms of changes depend on the spatial distributions of microenvironments, the strength of selection and the amounts of dispersal (see also SOKAL 1979; EPPERSON 1989). In addition, SOKAL, JACQUEZ and WOOTEN (1989) showed that immigrations into the margins of a population can also change spatial autocorrelation.

The present paper reports results from the first theoretical study of how precise measures of spatial patterns of genetic variation within populations are changed by selection in the form of simple fitness differentials between genotypes, where fitnesses are inherent in the genotypes and do not depend on microenvironments. The results show that in populations with limited dispersal, directional selection greatly reduces the patch sizes and both spatial and temporal correlations of genetic variation to degrees that should be easily detected in spatial samples from natural populations. Selection is simulated as differences in competitive ability among neighboring genotypes, and thus there are nonuniform probabilities for replacement genotypes for selectively removed

TABLE 1

Descriptions of simulated populations in sets sharing the same parameter values for mating system, N, selection, s, and immigration-mutation, μ

Set	N^a	s	μ	q^b	Number of populations run	Symbol on figures
1A	9	0.0	0.0	0.5	6	○——○
1B	9	0.0	0.0	0.1	3	○——○
2	25	0.0	0.0	0.5	4	●——●
3	9	0.01	0.001	0.0	4	□——□
4	9	0.0	0.001	0.0	4	■——■
5A	9	0.01	0.01	0.5	4	△——△
5B	9	0.01	0.01	0.0	4	△——△
6	9	0.0	0.01	0.0	4	▲——▲
7	9	0.10	0.001	0.0	6	○ - - ○
8	9	0.10	0.01	0.0	4	● - - ●

[a] Number of potential pollen donors including self, for interior locations.

[b] Initial probabilities of allele frequencies for generation zero.

individuals. Selection must commonly take this form in the many plant and animal populations where dispersal is very limited. The simulations also illustrate the changes in spatial patterns and temporal correlations that are brought about by nonselective random replacement processes, such as spatially uniform immigration, long distance gene flow, and mutation.

METHODS

Description of simulations: Monte Carlo simulations were conducted using a program written in FORTRAN. Each simulated population consisted of 10,000 genotypes located on a 100 × 100 square matrix or lattice. Simulation runs with selectively neutral genotypes were initialized by randomly choosing genotypes with probabilities that were binomial square proportions of the input allele frequencies, which were either 0.5 or 0.1. Almost all of the simulations with selection and immigration-mutation were initialized with the advantageous homozygote fixed in the populations. Simulation runs which shared the same amounts of selection and immigration-mutation, and mating system were replicated in sets of 4 to 9 (Table 1). The sequences of random numbers that were used to make choices in mating, selection, and immigration-mutation differed for each run. The linear congruential method was used to generate random numbers from a uniform (0, 1) distribution and these were partitioned to correspond to the probabilities of different prescribed possible outcomes. Thus the initial distributions and the sequences of choices in mating etc. should bear little similarity between different runs.

The life cycle was repeated at least 200 generations for each run. Through the mating stage of each simulated life cycle generation, the female parent of an offspring at each location was always the individual that occupied that location. For the simulation runs in sets 1, 3, 4, 5, 6, 7, and 8, pollen parents were chosen from one of the eight nearest neighbors, or from the same (maternal) plant with uniform probability one-ninth (thus selfing occurred with probability one-ninth). Exceptions to this rule were the boundary locations where mate choices were "reflected" against the boundary. Thus for single boundary locations (*i.e.*, not one of the four corners) each of the five neighbors had a one-sixth chance of being the pollen parent, and selfing occurred with probability one-sixth. One set of runs (set 2) differed in that pollen parents were chosen with equal probabilities from the 24 nearest neighbors and self; thus there was a 1/25th chance of self-fertilization, for interior locations. Mate choices were with replacement; progeny were kept in a holding matrix until all choices were made based on the parental spatial distribution. Whenever a parent was a heterozygote a random number was used to choose between the two alleles. These and other details of the mating cycle algorithm followed those in ROHLF and SCHNELL (1971) and SOKAL and WARTENBERG (1983). Throughout the present work we refer to the populations as plant populations, but the same processes described here might occur in animal populations that have uniparental dispersal and self-fertility. Moreover, details of dispersal seem to be relatively unimportant; rather it is the total variance of dispersal distances that primarily determines spatial distributions produced in limited gene flow models (see WRIGHT 1946; SOKAL and WARTENBERG 1983).

In simulation runs that included immigration-mutation, genes in the chosen gametes were changed to the opposite allele with probability μ, before the zygote was formed. This simulated any of: (1) effectively uniform long distance ovule and pollen migration from residents within the population; or (2) uniform immigration from an outside source; or (3) random reversible mutation with (high) equal rates.

Next in the simulated life cycles of some sets of runs (set 3, set 5, set 7, and set 8; see Table 1), selection was simulated to act on the progeny. Genotypes *AA*, *Aa*, *aa* were removed with additive probabilities 0, $s/2$, s. Removed individuals were replaced with the same regime of probabilities as for the pollen parent choice; replacements were chosen at random from the nearest eight neighbors, and "self-replacement" occurred with one-ninth probability (for interior points). Again replacements were chosen "with-replacement" by using a holding matrix for the post-selection populations. Selection in these models behaves like competition between neighboring plants, and is an appropriate form for populations that have low levels of dispersal. We note that this form of selection in the simulations effectively introduces some local migration of diploids, but the levels are so low that such migration, without a "directional" (*i.e.*, against the deleterious gene) component, has negligible effects on the genotypic distributions. The spatial patterns produced would probably be negligibly affected if the ordering of mutation, selection, and mating were changed.

Statistical measures of genetic structure: For each ten generation increment of each simulation run, the population (at the "juvenile" stage of the life cycle, *i.e.*, just after mutation and mating, prior to selection) was characterized in several ways. First, the allele frequency and Wright's fixation index were calculated for the lattice of 10,000 genotypes. Then the lattice was subdivided into 400 contiguous quadrats of size 5 by 5, and the allele frequency, q_i, in each quadrat i was calculated and recorded along with quadrat location in the 20 by 20 matrix or lattice of quadrats, also referred to as a gene frequency surface. Pairs of quadrats were grouped by the Euclidean distances between

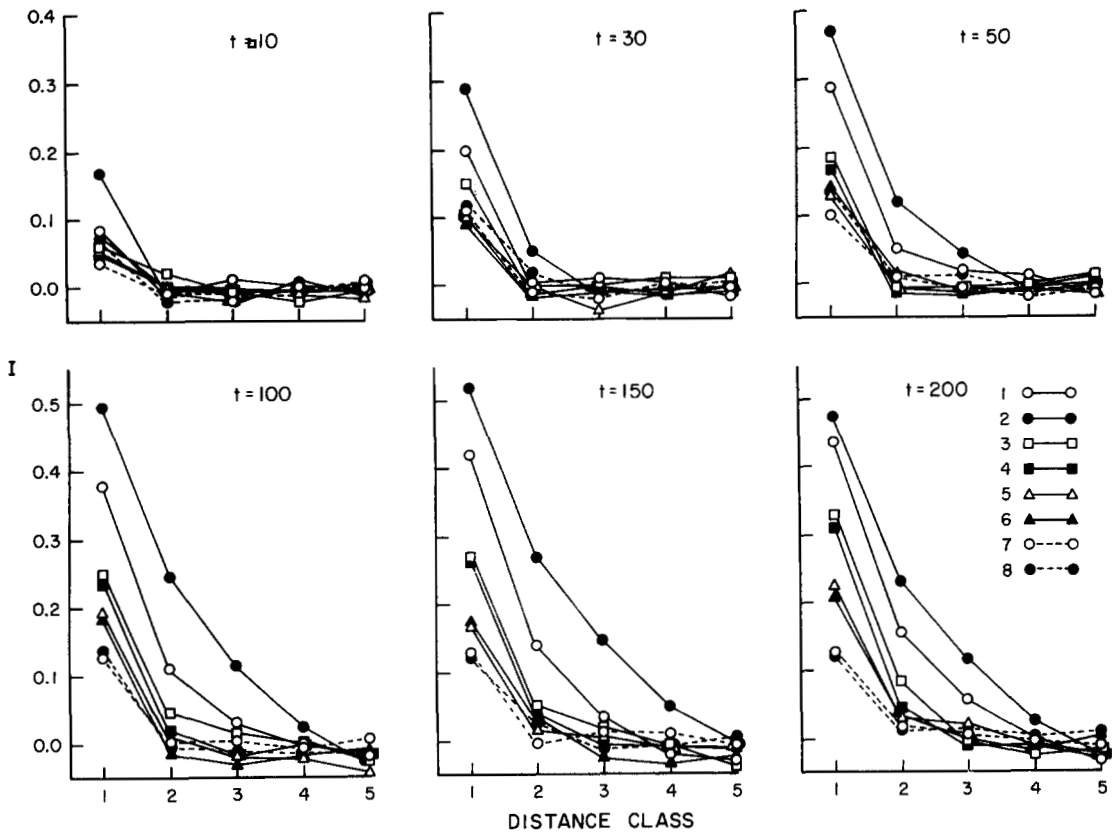

FIGURE 1.—Average *I*-correlograms (averages of Moran's *I*-statistic for each of the first five distance classes) for each set of simulations, at different generations, *t*. See Table 1 and text for definition of sets. Distance classes are in quadrat lengths on a 20 × 20 lattice of gene frequencies in quadrats of 25 individuals (size 5 × 5).

the quadrat centers. Thus distance class k contained all pairs of quadrats that were separated by $k - 0.5$ to $k + 0.5$ (for $k = 1,2, \ldots, 27$) quadrat lengths (equals $5k - 2.5$ to $5k + 2.5$ unit lengths between adjacent plants on the original genotypic lattice). Moran's I-statistic for the kth distance class was calculated by:

$$I_k = n \sum_i \sum_j z_i z_j / (W_k \sum_i z_i^2),$$

where $z_i = q_i - q$, and q is the mean of the quadrat allele frequencies in the population (SOKAL and ODEN 1978a; CLIFF and ORD 1981). The summation is taken over all pairs of quadrats that fall into distance class k, and W_k is twice the total number of pairs of quadrats in k. Graphs of the *I*-statistics for each of the distance classes are termed correlograms.

Join-count statistics were calculated on some of the genotypic surfaces of simulations at generation 200. The statistics were calculated for samples with size n from these surfaces, because excessive computations are required to compare all (10,000) × (9,999)/2 pairs of individual genotypes. Most of these samples were structured samples from the entire populational area, in other cases the samples represented complete censusing of subareas of populations. Briefly, join-count statistics were calculated as follows. First, distance classes, k, were formed for each multiple of the number of genotypic lattice units separating nearest neighbor sample genotypes. The $n(n - 1)/2$ pairs of sample genotypes were placed into these classes. The genotypes of individuals at two locations defined a join. Thus $n_{ij}(k)$ is the number of joins between genotypes i and j in distance class k. Each type of join was compared to its expected value under the null hypothesis, H_0, that the sample genotypes are randomized with respect to locations (CLIFF and ORD 1981). Under H_0 the expected value of $n_{ij}(k)$ is $\mu_{ii}(k) = W_k n_i(n_i - 1)/2n(n - 1)$, and $\mu_{ij}(k) = W_k n_i n_j/n(n - 1)$, for $i \neq j$. Here n_i is the number of plants with genotype i in the sample and W_k is twice the total number of pairs of points in class k. The standard errors, $SE_{ij}(k)$, of $n_{ij}(k)$ under H_0 are given for example in CLIFF and ORD (1981) and SOKAL and ODEN (1978a). The statistic $\mathrm{SND}_{ij}(k) = [n_{ij}(k) - \mu_{ij}(k)]/SE_{ij}(k)$, is distributed asymptotically as a standard normal deviate, under H_0 (CLIFF and ORD (1981).

RESULTS

Spatial autocorrelation: Strong selection ($s = 0.10$) and immigration-mutation retard development of spatial autocorrelations, as can be seen in the first five distance classes of the set-mean *I*-correlograms (graphs of *I*-statistics by distance class) for each set of simulation runs for different generations (Figure 1). Differences among the sets were greatest for the *I*-statistics for the first distance class, I_1. Values of I_1 differed significantly for all generations tested, using ANOVA and Duncan's multiple range tests (Table 2). The largest differences among the sets occurred during the period between 100 to 200 generations. The *I*-statistics for sets 3 and 4 (Figure 1) are slightly smaller than for set 1; this indicates that with $\mu = 0.001$, mutation or immigration has little effect on spatial

TABLE 2

Means and standard deviations (in parentheses) of *I*-statistics for runs within the same set, and Duncan's multiple range tests for differences in values of *I*-statistics among the sets of simulations for a given distance class and at a given generation time (*t*)

		Set[a]							
I	t	1	2	3	4	5	6	7	8
I_1	10	0.083 B (0.033)	0.170 A (0.020)	0.053 B (0.043)	0.050 B (0.029)	0.060 B (0.014)	0.080 B (0.019)	0.045 B (0.020)	0.063 B (0.021)
I_1	30	0.199 B (0.030)	0.288 A (0.017)	0.153 C (0.048)	0.105 CD (0.021)	0.105 CD (0.035)	0.093 D (0.015)	0.112 CD (0.017)	0.115 CD (0.011)
I_1	50	0.288 B (0.041)	0.370 A (0.046)	0.185 C (0.047)	0.168 C (0.013)	0.133 CD (0.022)	0.140 CD (0.029)	0.102 D (0.045)	0.138 CD (0.026)
I_1	100	0.377 B (0.032)	0.495 A (0.023)	0.250 C (0.021)	0.233 CD (0.039)	0.190 D (0.043)	0.190 D (0.021)	0.128 E (0.034)	0.135 E (0.015)
I_1	150	0.422 B (0.040)	0.518 A (0.032)	0.273 C (0.061)	0.273 C (0.022)	0.170 D (0.024)	0.173 D (0.008)	0.132 D (0.035)	0.130 D (0.046)
I_1	200	0.437 A (0.051)	0.475 A (0.067)	0.330 B (0.062)	0.313 B (0.052)	0.225 C (0.021)	0.208 C (0.049)	0.132 D (0.014)	0.128 D (0.026)
I_2	200	0.163 A (0.068)	0.235 A (0.078)	0.085 B (0.059)	0.043 B (0.036)	0.038 B (0.031)	0.040 B (0.031)	0.018 B (0.033)	0.013 B (0.016)
I_3	200	0.059 A (0.062)	0.120 A (0.050)	−0.003 B (0.046)	−0.013 B (0.035)	0.018 B (0.031)	0.003 B (0.019)	0.008 B (0.030)	0.018 B (0.022)

[a] Sets which share a letter do not have significantly different means.

autocorrelation. Immigration-mutation with higher rates ($\mu = 0.01$) further reduces autocorrelations; at generation 200 the values of I_1 for set 5 and set 6 are only about one-half that for set 1 (Table 2).

Strong selection ($s = 0.10$) reduces I_1 to very small levels (Table 2). Set 7 and set 8 have values that are about one-half that of sets that have either weak selection (sets 3 and 5) or no selection (sets 4 and 6) and the same amount of immigration-mutation. These values are less than one-third those for the pure isolation by distance model (set 1). In contrast weak selection ($s = 0.01$) has little effect on spatial autocorrelation. The values of I_1 for set 3 and set 5 are only slightly smaller and not significantly different from set 4 and set 6, respectively.

Values of *I*-statistics for $k = 2$ and $k = 3$ generally followed the same pattern among the sets (*e.g.*, see for generation 200, Table 2), but the differences were not as large as those for $k = 1$. For distance class $k = 4$, there were almost never substantial differences among any of the sets 1, 3, 4, 5, 6, 7, and 8. Similarly, for the higher distance classes $k > 4$, the only differences are that runs in set 1 or set 2 have slightly more negative correlations. For all sets, the *I*-statistics for $4 < k \leq 27$ were, in general, slightly less than zero; thus these classes were not very informative and will not be discussed further.

The *I*-correlograms for simulations with greater distances of pollen dispersal (set 2) were larger (*i.e.*, the *I*-statistics for small k were larger) than for set 1. Although the values of I_1, I_2, I_3 for set 2 at generation 200 do not differ significantly from those for set 1, values of I_1 for set 2 were significantly greater at generations 10, 30, 50, 100 and 150 (Table 2). Thus, the increased dispersal in set 2 results in a small increase of autocorrelation. Nonetheless, these results suggest that autocorrelation is relatively insensitive to differences in pollen dispersal distances within the ranges for the simulations in set 1 and set 2. The mating system in set 1 is essentially identical to simulation "set 1 and set 2" of SOKAL and WARTENBERG (1983), and these have very similar correlograms. The *I*-correlograms for set 2 are slightly smaller than those for another model in SOKAL and WARTENBERG (1983) that had biparental dispersal from the same-sized (25 potential parents) neighborhood (see also EPPERSON 1989).

The means of the spatial autocorrelation statistics differ significantly between some sets, but there is further issue of how replicable these differences are for populations that have different values of the parameters s and μ. High replicability was evident throughout, for example in the small values of the standard deviations of I_1 for runs within each set (Table 2). The spread of *I*-correlograms are typified by those shown in Figure 2 for set 1 and Figure 3 for set 7. Similar replicability was found for distance class $k = 2$, but differences were less dependable for distance classes $k \geq 3$. An UPGMA cluster analysis of the Manhattan distances (sum of the absolute differences for I_1 through I_5) between pairs of the *I*-correlograms at generation 200 showed that runs generally were grouped with other runs of the same set, and less frequently with runs of certain other sets. In particu-

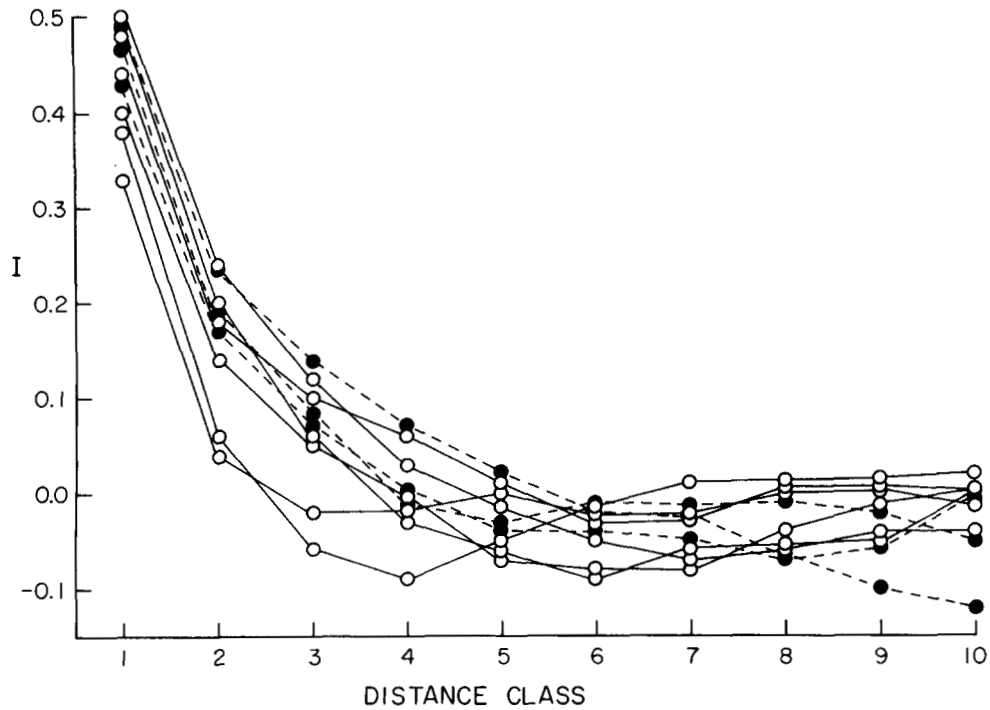

FIGURE 2.—*I*-correlograms for the nine replicate simulations in set 1. Replicates differed in initial allele frequencies, q_0: O–q_0 = 0.5; ●–q_0 = 0.1.

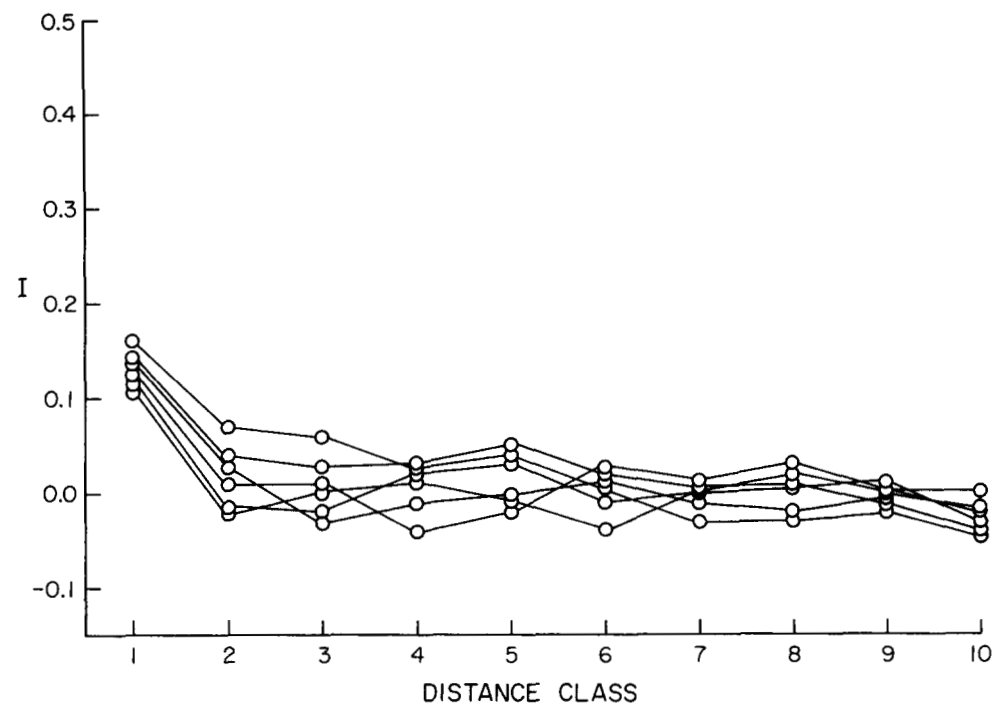

FIGURE 3.—*I*-correlograms for the six replicate simulations in set 7.

lar, runs in set 1 were sometimes grouped with those in set 2, likewise runs in set 3 with set 4, set 5 with set 6 and set 7 with set 8. Runs in other set combinations were almost never grouped together before groups had formed that contained all members of the same set combinations mentioned above. Similar clustering was observed when only values of I_1, or I_1 and I_2, were used. Thus there are diagnostic differences in spatial autocorrelation in simulated populations with isolation by distance only (sets 1 and 2), *vs.* those that have "low" (μ = 0.001) immigration-mutation (sets 3 and 4), versus those with "high" (μ = 0.01) immigration-mutation (sets 5 and 6), versus those which have strong (s = 0.10) selection (sets 7 and 8). The small differences attributed to weak selection were not replicable.

The stability of genetic structure is illustrated by the spatial autocorrelations at different generations. Autocorrelations for all sets (especially among sets 3–

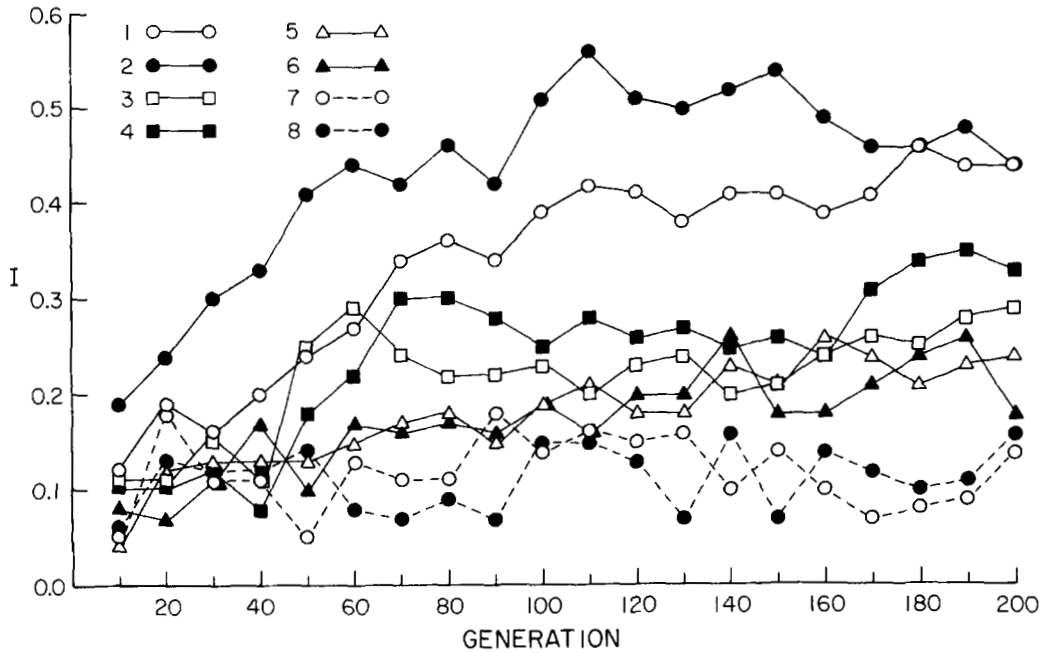

FIGURE 4.—Values of *I*-statistics for distance class one from each ten-generation increment of one replicate from each set.

8) were not pronounced at generation 10, but the same contrasts between sets that were replicable at generation 200 were also obvious by generations 30 or 50 (Figure 1, Table 2). Spatial autocorrelation in runs of sets 1 and 2 increased rapidly up until about generation 100, and afterwards changed little. This fits with visual inspection of the surfaces, which indicate that the populations of sets 1 and 2 have formed large stable groups of homozygotes prior to about generation 100. Thus the spatial autocorrelation or genetic structure of these populations had stabilized or reached a "quasi-stationary" state (SOKAL and WARTENBERG 1983). We note that this does not mean that a surface does not change; gene flow can cause changes in areas between opposite type patches, and visual inspection indicated that patches slowly changed locations (see results on temporal correlations).

Correlograms for runs of sets 5 and 6 changed very little after generation 50, and runs with strong selection (sets 7 and 8) changed little after the 30th generation. This suggests that the patch structure of these populations had also stabilized earlier. Here structure may have reached a true stationary state, because mutation greatly reduces the rates to regional fixation and precludes global fixation. The decrease of rates of increase of autocorrelations up to a point in time, and the subsequent amounts of fluctuations for individual runs are illustrated in Figure 4.

The mean correlograms for sets 3 and 4 continued to increase through to generation 200. This was largely due to one or two of the runs within each set, whereas most other runs showed little change (see, *e.g.*, Figure 4) after about the 100th generation. It is likely that because immigration-mutation is rare ($\mu = 0.001$) and selection ineffective ($s = 0$, or 0.01), stochastic events sometimes leave persistent imprints on the surfaces (see discussion below). Alternatively, it may simply be due to the fact that the allele frequencies in runs of sets 3 and 4 continued to steadily increase, unlike all other sets.

Differences in allele frequencies, q, had virtually no effect on either spatial autocorrelations or patch sizes (see discussion below). Autocorrelations for runs in set 1 that had initial frequency, q_0, of about 0.10 were not distinguishable from those with $q_0 = 0.50$ (see, *e.g.*, Figure 2). The effects of frequency were also negligible in the isolation by distance simulations of SOKAL, JACQUEZ and WOOTEN (1989). Nor does frequency seem to be a factor for the simulations with selection and immigration-mutation. Runs in set 7 *vs.* set 8, set 3 *vs.* set 4, and set 5 *vs.* set 6, had nearly identical spatial autocorrelations, even though they had different allele frequencies (see Figure 8). Thus, lower frequencies seem to have been accompanied by fewer patches rather than by smaller patches. This is supported through visual inspection of surfaces. In other words, fewer random immigration-mutation events apparently resulted in smaller numbers of patches. This result also suggests that patches evolve more or less independently of each other in these simulations. In sum, these results suggest that the differences in spatial autocorrelation among the simulated populations depend directly and strongly on the parameter s, and less so on the parameter μ.

In summary, both strong selection and high rates of immigration-mutation retard the development of

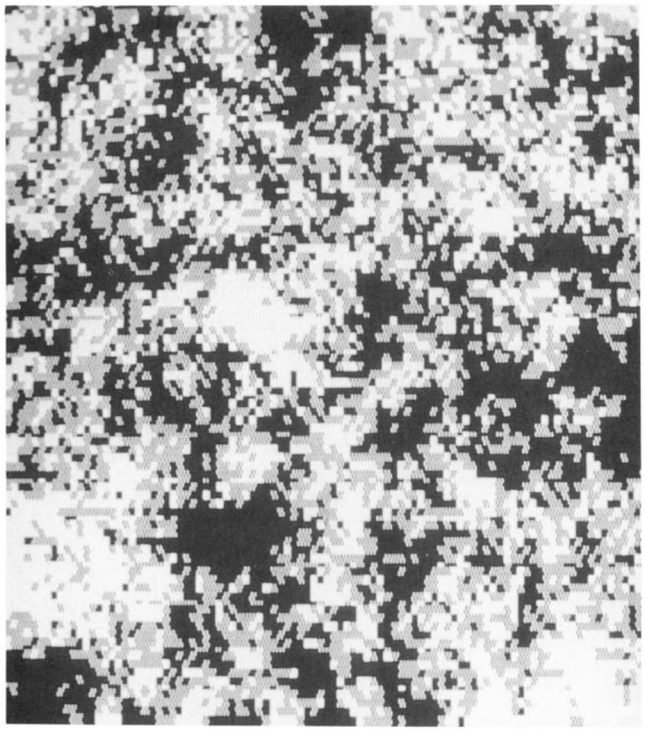

FIGURE 5.—Spatial distribution of genotypes in one replicate of set 1 at generation 200: □, ▨, ■ = for genotype *aa*, *Aa*, and *AA*, respectively.

spatial autocorrelation. Strong selection also reduces the amount of autocorrelation during phases of stable structure, which are quickly reached. High immigration-mutation rates act similarly, but overall have lesser effects, and thus longer periods are required to stabilize population structure. Weak selection and low immigration-mutation both have little effect.

Patch sizes: An important measure of spatial patterns is the distance at which *I*-correlograms become negative, the *X*-intercept (SOKAL and WARTENBERG 1983). For simulated populations with isolation-by-distance only, the *X*-intercept is roughly equal to the (average) diameter of patches, or areas containing mostly one of the homozygotes. Figure 5 shows a genotypic surface for one of the simulations of set 1 at the 200th generation, and Figure 6 shows the correlograms of the (asymptotically) standard normal deviate (SND) statistics (which test observed numbers of joins between different pairs of genotypes, at different distances of separation, against the null hypothesis, H_0, that sample genotypes are randomized with respect to location; see discussion in METHODS). For example, positive values greater than 1.96 for joins between two individuals with *AA* genotypes, mean that *AA* genotypes are correlated at the given distance class. (In this example, only every other row and column of the 100 by 100 lattice of genotypes was included in the calculations in order to reduce the amount of calculation.) The distance classes in Figure 6 were multiples of 2 genotypic lattice units (0.4 quadrat units), and are expressed in genotypic lattice units. Joins of types $AA \times AA$ and $aa \times aa$ are in excess at distances up to about equal to the value of the *X*-intercept of the *I*-correlogram for the same surface. This was generally true for SND-correlograms calculated for several other simulations in set 1 at generation 200. Visual inspection of these surfaces (*e.g.*, see Figure 5) and those of set 2 at generation 200 verified that there were large areas in which there was almost perfect contiguity between like-homozygotes. Thus, under the present two models of mating by proximity, the *X*-intercepts for *I*-correlograms approximates the average diameter of patches of homozygotes. However, it seems possible that the *X*-intercepts of *I*-correlograms may differ from patch diameters under mating models that have different dispersal.

Numerical values of *X*-intercepts of the *I*-correlograms were obtained by interpolating between distance classes. Such values for set 1 (Table 3) are very close to those found by SOKAL and WARTENBERG (1983), and as expected the values for set 2 are slightly larger. The set mean values of *X*-intercepts for *I*-correlograms rarely differed statistically for any given generation, according to ANOVA and Duncan's multiple range tests calculated on the ranks of the *X*-intercepts among all 39 simulations (Table 3). This contrasts the marked reduction for sets 3–8 of *I*-statistics for short distances (Table 2). However, the mean *X*-intercepts for sets 3–8 were consistently lower than for set 1 over all generations. Thus, it appears that selection and mutation did slightly reduce the *X*-intercepts. The set mean values of *X*-intercepts of sets 3 through 8 were much lower (up to 50% lower) than set 1 in the earlier generations; but at generation 200 reductions were less than 22%. The standard deviations for *X*-intercepts for runs within sets were often large for sets 3–8, and this was due usually to a single outlier which had much larger *X*-intercepts than other runs in the same set. For example, the *X*-intercept of one run in set 6 at generation 200 was 5.75 compared to a mean of 2.30 for the other three runs in this set. Outlier correlograms often raised the mean correlograms to positive values for distance classes $k = 3$ to 6, and hence inflated the *X*-intercepts of the average correlograms (Table 3). Such outliers generally had small positive *I*-statistics (usually less than 0.03) for $k = 3$ up to 5 or 6. These values do not indicate much autocorrelation, and do not seem to measure correlations within any well defined patch structure. Rather, visual inspection of the surfaces with strong selection (*e.g.*, see Figure 7) and/or high rates of random replacement suggests that they measure slight concentrations of relic patches of the rare types within larger areas; these may have resulted from stochastic events (see discussion below).

To further examine the effects of selection and

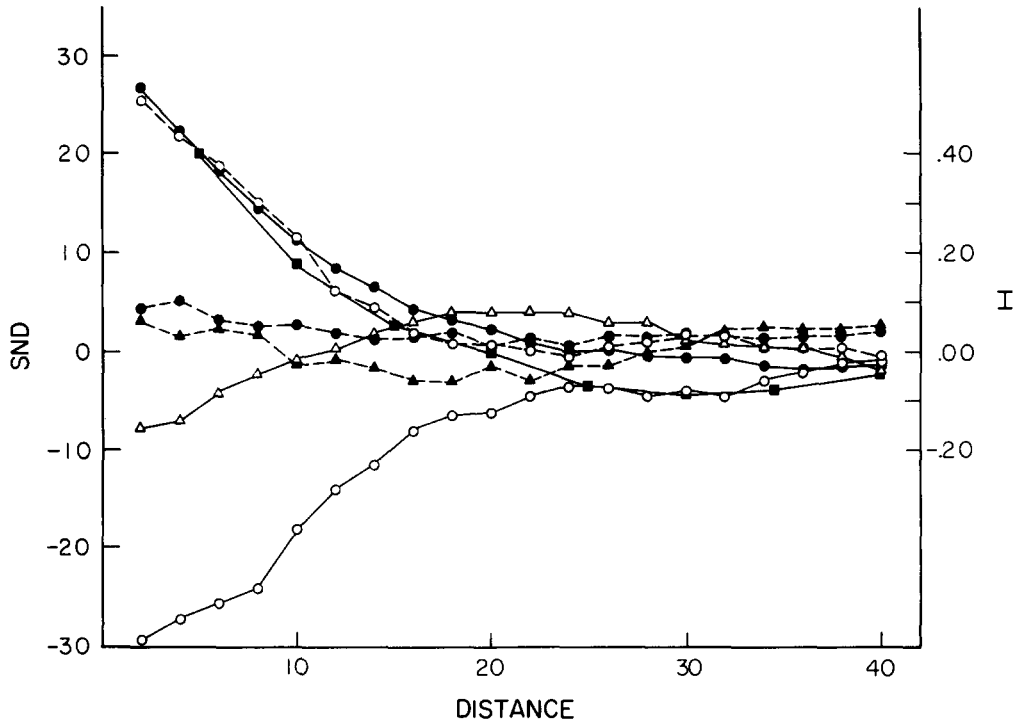

FIGURE 6.—Correlograms of SND join counts of pairs of genotypes and Moran's *I*-statistics for the spatial distribution shown in Figure 5. *Key:*

●—● *AA* × *AA* △—△ *AA* × *Aa*
○----○ *aa* × *aa* ▲----▲ *aa* × *Aa*
○—○ *AA* × *aa* ■—■ *Moran's I*
●----● *Aa* × *Aa*

immigration-mutation on the scale of patch structure, it is informative to partition out small positive correlations. The (interpolated) distances at which the set-mean correlograms intercept with the values $I = 0.02$ and $I = 0.05$ are given in Table 4 (see also Figure 1). The 0.05 intercepts for sets 3, 4, 5, 6 (and to a lesser degree sets 7 and 8) are reduced far below the values of *X*-intercepts for these sets (Table 3), especially after the 100th generation. In contrast, the $I = 0.05$ intercepts for sets 1 and 2 are not much smaller than the *X*-intercepts for these sets. As a result, at generation 200 the 0.05 intercepts for sets 3–8 are about 30–50% smaller than that of set 1. Moreover, the pattern in which the set mean correlogram intercepts with 0.05 increase with time for the different sets corresponds closely to the pattern seen in increases in values of I_1, I_2, and I_3. Assuming that patch structure is the primary determinant of values of *I*-statistics for these distance classes, this correspondence suggests that the *I* correlogram intercepts with 0.05 are very close to the true diameters of patches of homozygotes; this was further supported by visual inspection of the surfaces. Differences among sets for the 0.02 intercepts are intermediate between those for *X*-intercepts and those for the 0.05 intercepts.

Once the small correlations are partitioned out, it is clear that when selection was strong (sets 7 and 8) an equilibrium patch size was quickly established (within 50 generations). This is interpreted as an equilibration of the stochastic spread of descendents of new mutants over local areas with the effects of selection in eroding patches of mutant types. Relic concentrations were emphemeral but raised *X*-intercepts temporarily. Such fluctuations were evident in the *X*-intercepts of individual runs (results not shown), and in the mean *X*-intercepts in set 7 and set 8. For sets 4, 5, and 6 the intercepts with 0.05 continued to increase slightly up to about generation 100 or 150. Those of set 3 increased up to the termination of the simulations, but the *X*-intercepts for these sets also increased. Weak selection was ineffective at completely removing patches of deleterious genotypes. Hence the effects of repeated chance proximal positioning of patches or patch remnants may have persisted for longer periods and accumulated.

Dynamics of genotypic frequencies: Allele frequencies, q, changed little during the neutral simulations, set 1 and set 2 (Figure 8), as expected for a neutral equilibrium in a large population. In contrast, q approached apparent equilibrium values rapidly for

TABLE 3

Mean values (X) and standard deviations (in parentheses) of X-intercepts for individual simulation runs within sets, and X-intercepts of the average I-correlogram for each set (X_{AVE})

Parameter	Generation	Set 1	2	3	4	5	6	7	8
X	50	4.01 (1.66)	4.83[a] (2.97)	2.61 (1.10)	2.59 (1.20)	1.51 (0.41)	3.16[a] (1.53)	2.64 (0.78)	2.52 (0.99)
X_{AVE}	50	4.40	3.90	1.98	1.94	1.94	2.56	2.50	3.57
X	100	4.00 (1.14)	5.57[a] (2.71)	3.59 (0.62)	3.09 (1.69)	2.16 (0.35)	2.07 (0.37)	2.30 (0.76)	2.28 (0.57)
X_{AVE}	100	3.82	3.82	4.00	2.47	2.20	1.93	3.71	1.98
X	150	3.91 (0.84)	5.61 (1.66)	3.15 (1.24)	4.43[a] (3.08)	2.67 (0.64)	2.59 (0.56)	2.42 (1.16)	2.73 (0.80)
X_{AVE}	150	3.69	4.86	3.67	2.83	3.44	2.55	1.98	2.58
X	200	3.99 (0.95)	4.97 (0.89)	3.39 (0.83)	3.31 (1.59)	3.10 (0.88)	3.83[a] (1.57)	3.78[a] (2.07)	3.14 (1.18)
X_{AVE}	200	4.03	4.61	2.97	2.76	3.58	3.13	6.29	4.50

[a] Set contained one simulation that had an X-intercept that was much longer than others in the same set.

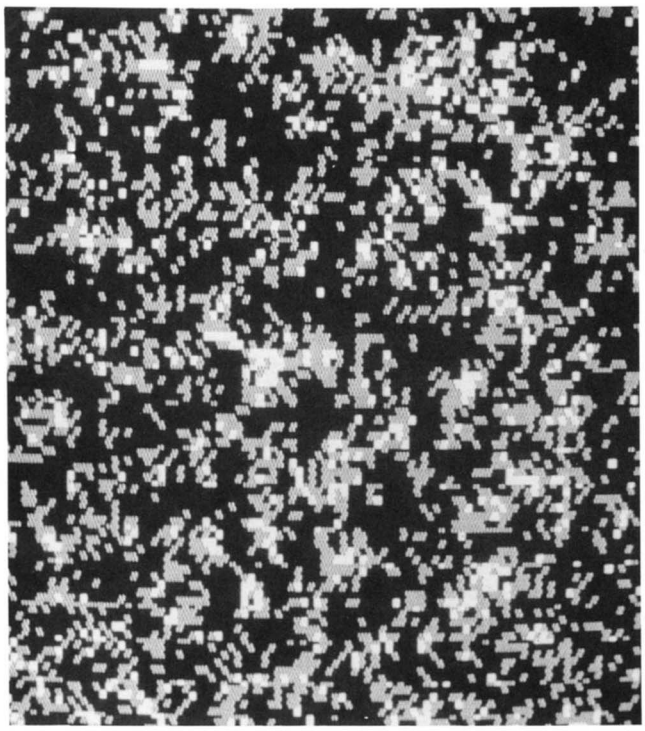

FIGURE 7.—Spatial distribution of genotypes in one replicate of set 7 at generation 200: □, ▨, ■ = for genotypes *aa*, *Aa*, and *AA*, respectively. Allele *a* is selected against.

sets with strong selection (set 7 and set 8), and somewhat more slowly in simulations with high rates of immigration-mutation and with either weak selection or no selection (set 5 and set 6). Individual runs of set 5 initialized with either $q_0 = 0$ or $q_0 = 0.5$ evolved to the same value by generation 170 (Figure 8). It is noteworthy that the times at which allele frequencies stabilized in these sets were coincident with the times at which spatial structure stabilized. Again this is consistent with the idea that a balance is reached between the local stochastic spread of deleterious genotypes and removal by selection, and that the resulting sizes of patches differ among the sets.

TABLE 4

Intercepts of average correlograms with the (A) $I = 0.02$ value and (B) $I = 0.05$ value

	Generation	Set 1	2	3	4	5	6	7	8
(A)	50	3.0	3.5	1.9	1.8	1.7	1.9	1.8	1.9
	100	3.3	4.1	2.8	2.0	1.9	1.8	1.9	1.8
	150	3.3	4.6	3.0	2.5	2.0	2.2	1.8	2.0
	200	3.6	4.2	2.7	2.5	2.8	2.5	2.0	1.9
(B)	50	2.0	2.9	1.7	1.7	1.5	1.7	1.5	1.7
	100	2.8	3.7	2.0	1.9	1.8	1.7	1.6	1.6
	150	2.9	4.0	2.1	2.0	1.8	1.9	1.6	1.7
	200	3.2	3.8	2.3	2.0	1.9	2.0	1.7	1.6

The average fitnesses of genotypes depended on the frequencies of genotypes among their competing neighbors, and therefore depended somewhat on structure. In order to examine the effects of structure on the efficacy of selection, the dynamics of allele frequencies, q, can be compared to those of frequencies, q^*, in mathematical models of mutation-additive selection (with fitness parameter s^*) in infinite populations with random mating. (Note that inbreeding *per se* is unimportant because the probabilities of selective removal were additive.) We set $s^* = 8s/9$, because "removed" individuals were "replaced" by themselves with probability one-ninth (in the interior locations). The results of these calculations can be easily summarized: for every generation for all simulations, $\Delta q = q - q^*$ was less than 0.02. However, among populations with selection, Δq was greatest for

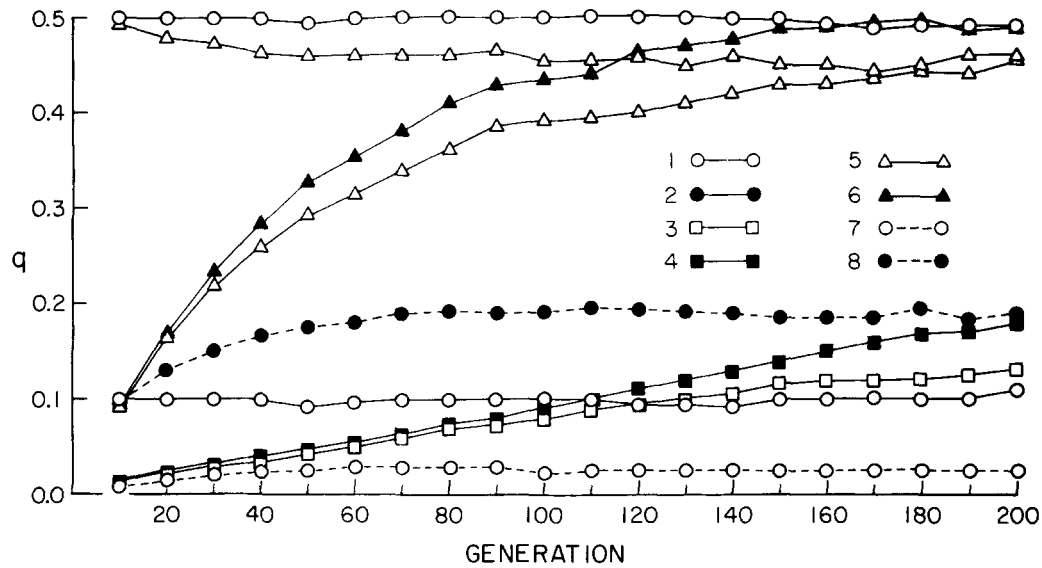

FIGURE 8.—Average allele frequencies for sets (or subsets) for each ten-generation increment. For sets 3, 4, 6, 7 and 8, the initial allele frequencies were $q_0 = 0$. For set 2 and subset 1A, $q_0 = 0.5$; for subset 1B, $q_0 = 0.1$. For subset 5A, $q_0 = 0.5$; for 5B, $q_0 = 0$.

those with weak selection and hence greater structure, both prior to and after (for sets in which equilibrium was reached, sets 5, 6, 7, and 8) apparent equilibrium was reached. Thus structure does appear to have an effect, however small. It is worth noting that in simulations with no selection, but with immigration-mutation (sets 4 and 6) q initially increased slightly faster than in the mutation model for panmictic populations, but in set 6 q stabilized once the predicted value 0.5 was reached. In set 4 the mutation rate was too small for equilibrium to be reached within 200 generations.

Wright's fixation index, F (WRIGHT 1965), for runs in set 1 increased rapidly from near zero at generation 0 up until about the 10th generation, then it increased more slowly (Figure 9). After about generation 100, F increased very little, probably because spatial autocorrelation stabilized after about 100 generations. The values of F for generations 100 and 200 (0.32, 0.33 respectively) are much greater than the value predicted for the mixed mating model for a population of infinite size, $F_e = (1 - t)/(1 + t)$; with the outcrossing rate, t, approximately equal to 8/9, $F_e = 0.06$. The difference is primarily caused by consanguinous outcross mating, via mating by proximity and spatial autocorrelations. Similarly, for set 2, F rapidly approaches 0.15, which is much greater than the predicted F for the mixed mating model with t equal to 24/25, $F_e = 0.02$.

Strong selection (in set 7 and set 8) and high rates of mutations (in set 5 and set 6) each lower F considerably, and weak selection or low rates of immigration-mutation caused smaller reductions (Figure 9). This pattern follows the differences in spatial autocorrelation. Thus F is probably reduced, at least in large part, because of the lower amounts of structure in these populations, and thus lower frequencies of consanguinous matings. However, the both selective removal and random replacement of genotypes also affect F directly. For all sets the F statistics for individual runs were very close to the means for sets.

Temporal correlations: Stability of the spatial distribution of genotypes over time depends on dispersal, the spatial genetic structure, and the regime of selection and immigration-mutation. The issue of such stability differs from the question of stability of the spatial genetic structure or autocorrelation. One measure of stability of the surface of genotypes over time is the correlation between the two matrices (or lattices) of allele frequencies in quadrats at different generations. Temporal correlations were calculated between the matrices for generations 50, 100, 150 and 200 and those for all earlier generations at ten-generation increments. The differences in temporal correlations between the sets are illustrated by the set means of Fisher's Z-transform of the matrix correlation coefficients for comparisons involving generation 200 (Figure 10). For all sets, the temporal correlations were very uniform for simulation runs in the same set. Thus, the differences seen in the set mean temporal correlations distinguish the different processes of selection and immigration-mutation.

Greater levels of dispersal per generation in set 2 caused lower temporal correlations than for set 1, especially for the shorter time lags. The correlations for set 1 are completely consistent with the results of SOKAL and WARTENBERG (1983), and as expected the correlations for set 2 are greater than those for the 25 biparental dispersal model of SOKAL and WARTENBERG. For time lags exceeding 70 generations, there are little differences between the two sets. In these

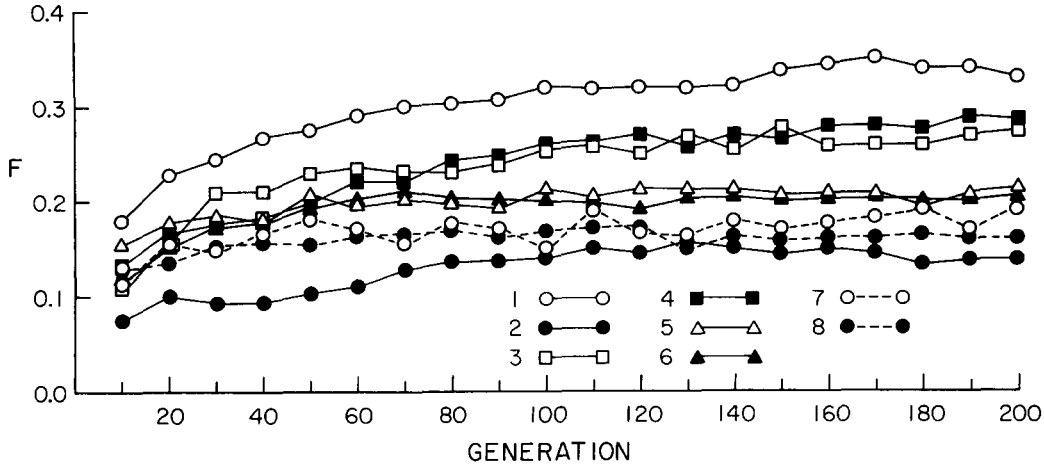

FIGURE 9.—Average values of Wright's fixation index, F, for each set for each ten-generation increment. Values of F were approximately zero in the initial generations of all simulations.

simulations correlations over long periods are probably primarily functions of the amount of relocation of patches. Thus, these results suggest that despite the greater short term gene flow in set 2, rates of patch relocation were similar to those for set 1.

Simulations with immigration-mutation only ($s = 0$) have much lower temporal correlations, especially for the shorter time lags (Figure 10). With $\mu = 0.01$ (set 6) values of Z for the ten generation lag are only about 50% as large as set 1, and with $\mu = 0.001$ (set 4) values of Z for lag 10 were about 80% as large. These reductions are probably too large to be accounted for by mutational change alone. They are probably due primarily to the stochastic spread of recent mutants, especially when these occur near the centers of patches of opposite type.

Selection with low intensity had little effect on temporal correlations; correlations are very similar for set 3 *vs.* set 4, and set 5 *vs.* set 6 (Figure 10). In contrast, strong selection greatly reduces temporal correlations. Comparing set 7 *vs.* set 4, and set 8 *vs.* set 6, the lag 10 correlations for generation 200 are nearly 50% lower for the sets with strong selection. Strong selection probably changes the surfaces over the short term by rapidly reducing and removing patches of deleterious genotypes.

Temporal correlations for generations 100 and 150 (results not shown) were nearly identical to those for the same time lag for generation 200, except that they were usually slightly smaller. This was true in the neutral simulations of SOKAL and WARTENBERG (1983). Among the present simulations, those with selection were more uniform than those without selection. This uniformity of lag correlations suggests that the forms of the structures in most of the simulations stabilize by about 50–100 generations. This follows from the fact that temporal correlations are determined by spatial correlations and the regimes of dispersal, immigration-mutation, and selection, and the regimes are essentially unchanging.

The temporal correlations are somewhat lower for the same time lags in the early generations for sets 1–6 (compare Figures 10 and 11). This probably occurred because the patch structures for these sets were still growing throughout the first 50 generations. At generation 50, the ranks of the average correlations among sets are similar to those for generation 200, except that some pairs of sets which have similar correlations at both periods, have switched ranks for some lags. The differences between the sets 3 through 8 are not as large. Nonetheless, both high rates of immigration-mutation and strong selection greatly reduce correlations compared to the pure isolation by distance model (set 1). In summary, these results show that temporal correlations are very sensitive indicators of selection and/or random replacement processes, regardless of age of populations.

DISCUSSION

Effects of selection on spatial-temporal patterns: The results of the simulations indicate that additive selection reduces structure of genetic variation within populations with limited gene dispersal far below levels expected for neutral loci when the fitness differential between opposite homozygotes is on the order of $s = 0.10$. Thus, spatial pattern analysis can be used to detect selection of this magnitude. These effects of selection on genetic structure are remarkable because fitnesses were not directly dependent on location. Strong selection or local competition between genotypes removed deleterious genotypes from the perimeters of patches of the deleterious homozygote. Such erosion initially retarded then stopped the increase of average patch sizes. By about the 30th generation the stochastic local spread of deleterious genotypes in new patches, following recurrent random immigration-

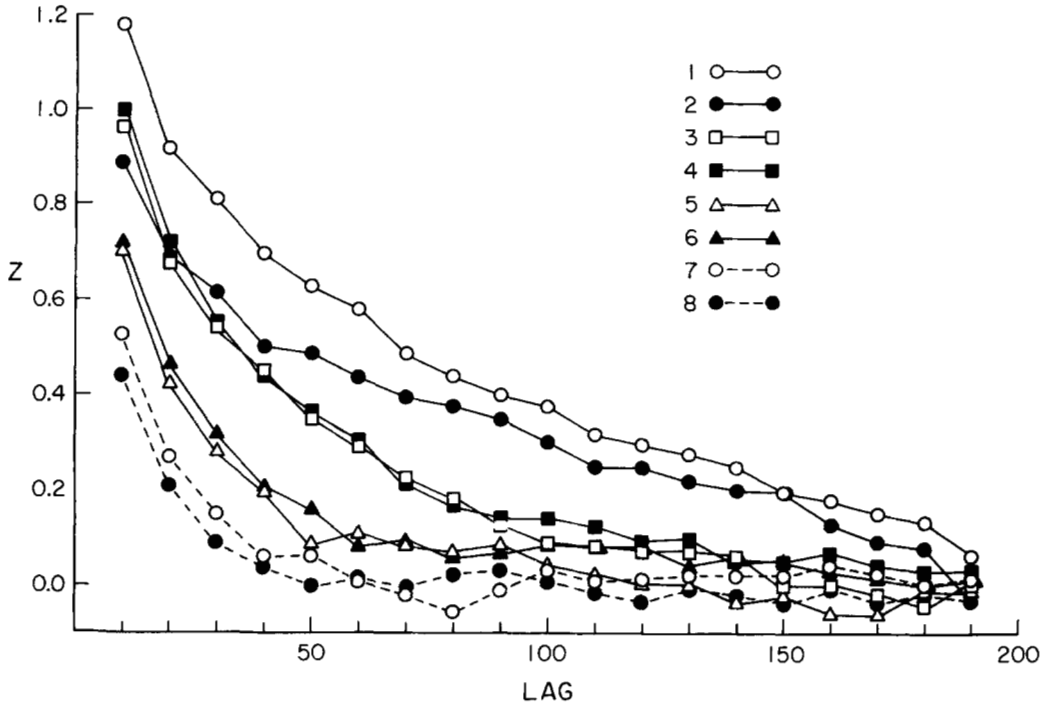

FIGURE 10.—Set averages of temporal correlations between generation 200 and all earlier 10-generation increments. Abscissa is Fisher's Z-transform of the average matrix correlation between the allele frequencies in quadrats for the two generations. Lag is the difference between a given generation and generation 200.

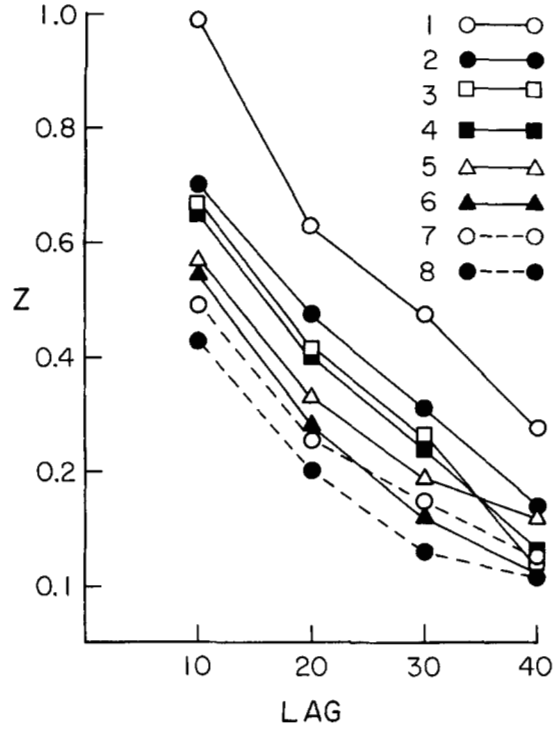

FIGURE 11.—Set averages of temporal correlations for ten-generation increment lags, with generation 50. See Figure 10.

mutation events, had equilibrated with the rate of removal of patches through selection. Patches averaged fewer than about 50 individuals, whereas patches in the neutral simulations averaged about 400–500. In simulated populations with even stronger selection, $s = 0.20$ (results not shown), all spatial autocorrelation statistics were near zero, including those for the first distance class; thus patches averaged fewer than about 25 individuals. In contrast, weak selection ($s = 0.01$) had negligible effects on spatial distributions.

Reductions in patch sizes were only weakly reflected in calculations of the intercepts of I-correlograms with zero (X-intercepts) for the populations with strong selection. However, in the cases for strong selection the values of I-statistics for distance classes 2–4 tended to be small and positive, and they probably were produced by ephemeral concentrations of patches or relics of patches within larger regions. The signs of empirical estimates of such small values of I are determined primarily by chance sampling error in spatial samples with moderate sizes. If such samples are spatially fine-scaled, and thus there are many distance classes between the small patch diameters for selected loci and the X-intercepts of correlograms for neutral loci, then the X-intercepts of sample correlograms for selected loci should be greatly reduced, and will more closely reflect the sizes of patches. The spatial distribution of small samples of genotypes of loci under selection may not differ significantly from random sampling.

Strong selection also increased the rates of change of the spatial distributions (*i.e.*, decreased temporal correlations) over short time periods, by speeding the removal or relocation of patches. The reductions in temporal correlations were large enough that they

should be easily detected in a multiple-locus study of populations sampled repeatedly over as little as ten generations. In contrast, for time lags greater than about 150 generations, the temporal correlations were near zero for all sets of simulations. Thus the spatial autocorrelations at the late generations may be nearly independent of initial or early spatial distributions.

The amounts of structure in the simulated populations with selection had little influence on either the rates of change or the equilibrium values of allele frequencies. Among these populations, even those with weaker selection and thus greater spatial autocorrelation, the frequencies of deleterious genes increased only slightly faster and reached slightly higher equilibrium values than for the panmictic models. Similarly in simulations with no selection, but with reversible equal mutation, structure had negligible effects on rates of increase of allele frequencies. Selection reduced values of Wright's fixation index, F, in a manner related to the selection-induced reductions of spatial autocorrelation. Values of F are determined primarily by the amounts of assortative matings that result from the combination of mating by proximity and spatial autocorrelations of genotypes (WRIGHT 1943; ROHLF and SCHNELL 1971; SOKAL and WARTENBERG 1983). The reductions of F caused by selection are probably due in large part to the lower amounts of structure (and hence less assortative mating) in populations with selection, although it is noted that additive selection also affects F directly.

Spatial structure may have different influences on both short and long term evolutionary changes in more complex situations. For example, with epistatic multilocus selection, the marginal fitnesses of single locus genotypes depend on values of linkage disequilibrium, which in turn depend in part on the spatial correlations of genotypes at different selected loci. Moreover, different forms of selection probably will produce a variety of changes in genetic structure. For example, quite different spatial distributions might be obtained with non-additive (*e.g*, asymmetrical overdominance) fitnesses.

Implications for studies of population genetics of natural populations: The results show that, under conditions where only short distance gene flow affects genetic structure within populations, the spatial autocorrelations of genotypes for different neutral loci should be similar, even if allele frequencies differ considerably among loci (see also SOKAL, JACQUEZ and WOOTEN 1989). Different loci should generally be subject to similar levels of dispersal. Moreover, even when neighborhood sizes vary by over an order of magnitude, patch structures are changed relatively little (SOKAL, JACQUEZ and WOOTEN 1989). Thus excessive reductions in spatial autocorrelations for some loci would indicate that natural selection may be operating on these loci.

Random replacement of genes with opposite alleles (without respect to location or genotype), caused moderate reductions of both spatial and temporal correlations when the rate of replacement, μ, was on the order of 0.01, but not when μ was on the order of 0.001. Clearly mutation cannot have much effect, with the possible exception of where mutator elements are frequent and highly active.

These results also provide a first approximation on the degree to which "random" or uniform immigration or long distance migration may reduce spatial autocorrelation for some loci relative to others. The uniformity aspect of the simulated processes must be commonly approximated in plant populations, because the probabilities of horizontal dispersal distances of pollen and seed are often nearly uniform for very long distances (LEVIN 1981). In such cases, for a diallelic locus with allele frequency q the expected total proportion of the genes in a population that are replaced by opposite alleles each generation is in the case of immigration $\mu = m(q + q_m - 2qq_m)$, and in the case of long distance migration $\mu = 2mq\ (1 - q)$. Here m is the uniform probability of replacement by a gene from a immigrant or long distance migrant, and q_m is the allele frequency in immigrants. The maximum of μ is 0.5 m for $q = 0.5$ for migration and $q = q_m = 0.5$ for immigration. Thus m must be on the order of 0.02 for there to be much effect on spatial patterns within populations. Even then immigration or migration *might* cause differences among loci only if the allele frequencies differ widely. The value of μ depends on allele frequencies and if q (or in the case of immigration also q_m) does not equal 0.5, then the probabilities of being replaced by an opposite allele from migrants will differ between the two alleles.

The effects of asymmetry of replacement cannot be addressed by the results of the present simulations. However, in the case of long distance migration, the dispersal parameter, m, could be combined with the dispersal variance for "short distance" dispersal in genetic isolation by distance models. Thus it seems that allele frequencies may be irrelevant with respect to the produced function of kinship on distance, $\phi(d)$ (see, *e.g.*, MALECOT 1973), and the related function of Moran's I on distance $I(d)$ (BARBUJANI 1987). For immigration, contrasts among loci may behave similarly, if the population is in interpopulational migration-drift equilibrium with all immigrant source populations, because values of $q + q_m - 2qq_m$ should be similar for all loci.

Finally, it should be noted that the dispersal of immigrants may be such that the margins of receiving populations are much more likely landing spots. In these cases the effects of immigration on genetic struc-

ture differ from those of the uniform replacement process simulated in the present study (SOKAL, JACQUEZ and WOOTEN 1989).

Application of results to populations of morning glory: In populations of the bumble bee-pollinated morning glory, *Ipomoea purpurea*, in the southeastern United States, homozygotes for a locus (*P/p*) that determines pink *vs.* blue flower color are spatially clustered into patch areas that contain an average of several hundred plants (EPPERSON and CLEGG 1986). Estimates of Wright's neighborhood sizes are in the range of 5–15 (ENNOS *and* CLEGG 1982). Dispersal distances of this magnitude produced similarly sized patches in simulated populations of selectively neutral genotypes (SOKAL and WARTENBERG 1983; SOKAL, JACQUEZ and WOOTEN 1989). It is remarkable then that in the same spatial samples of morning glory populations, white homozygotes (*ww*) for a locus that causes white flowers (locus *W/w*) were distributed either in much smaller patches or in a manner not significantly different from random sampling.

The gene that causes white flowered plants appears to be selected against in an manner similar to that modeled in the present simulations. The female and male reproductive success of plants with white-flower genes can be reduced by 10 percent or more compared to the fully colored homozygote (EPPERSON and CLEGG 1986, 1987a). This results from strong discrimination by pollinators against white homozygous morphs, and lesser discrimination against light heterozygous morphs (BROWN and CLEGG 1984; EPPERSON and CLEGG 1987a). Similar selection in simulations in sets 7 and 8 resulted in spatial distributions comparable to the white genotypes. Thus selection accounts for the observed distributions of white genotypes. There is no evidence of selection on locus *P/p*; and bumblebees visit blue versus pink flowers equally. Hence it is consistent that the distributions of pink *vs.* blue morphs fit the neutral simulations.

White genes may be maintained in low frequencies in populations of morning glories, because a mutator element can cause high rates of mutation at white loci (EPPERSON and CLEGG 1987b). However, the average mutation rates in populations are generally lower than 0.001; thus mutation alone cannot account for the reductions in spatial structure of white genotypes. It seems unlikely that immigration could have caused the repeated contrasts in distributions of genotypes at locus *P/p vs.* the white flower locus, in part because the genetic distances *between* populations are similar for the two types of loci (EPPERSON and CLEGG 1986).

This investigation was supported in part by National Science Foundation grant BSR-8418381 to M. T. CLEGG. The author thanks R. SOKAL and G. BARBUJANI for helpful comments on an earlier draft of the manuscript.

LITERATURE CITED

BARBUJANI, G., 1987 Autocorrelation of gene frequencies under isolation by distance. Genetics **117:** 777–782.

BROWN, B. A., and M. T. CLEGG, 1984 Influence of flower color polymorphism on genetic transmission in a natural population of the common morning glory, *Ipomoea purpurea*. Evolution **38:** 796–803.

CLIFF, A. D., and J. K. ORD, 1981 *Spatial Processes*. Pion, London.

DEWEY, S. E., and J. S. HEYWOOD, 1988 Spatial genetic structure in a population of *Psychotria nervosa*. I. Distribution of genotypes. Evolution **42:** 834–838.

ENNOS, R. A., and M. T. CLEGG, 1982 Effect of population substructuring on estimates of outcrossing rate in plant populations. Heredity **48:** 283–292.

EPPERSON, B. K., 1989 Spatial patterns of genetic variation within plant populations, pp. 229–253 in *Plant Population Genetics, Breeding, and Genetic Resources*, edited by A. H. D. BROWN, M. T. CLEGG, A. L. KAHLER and B. S. WEIR. Sinauer Associates, Sunderland, Mass.

EPPERSON, B. K., AND R. W. ALLARD, 1989 Spatial autocorrelation analysis of the distribution of genotypes within populations of lodgepole pine. Genetics **121:** 369–377.

EPPERSON, B. K., and M. T. CLEGG, 1986 Spatial autocorrelation analysis of flower color polymorphisms within substructured populations of morning glory (*Ipomoea purpurea*). Am. Nat. **128:** 840–858.

EPPERSON, B. K., and M. T. CLEGG, 1987a Frequency-dependent variation for outcrossing rate among flower color morphs of *Ipomoea purpurea*. Evolution **41:** 1302–1311.

EPPERSON, B. K., and M. T. CLEGG, 1987b Instability at a flower color locus in morning glory, *Ipomoea purpurea*. J. Hered. **78:** 346–352.

LEVIN, D. A., 1981 Dispersal versus gene flow in plants. Ann. Mo. Bot. Gard. **68:** 233–253.

MALECOT, G., 1948 *Les mathematiques de l'heredite*. Masson, Paris.

MALECOT, G., 1973 Isolation by distance, pp. 72–75 in *Genetic Structure of Populations*, edited by N. E. MORTON. University of Hawaii Press, Honolulu.

ROHLF, F. J., and G. D. SCHNELL, 1971 An investigation of the isolation-by-distance model. Am. Nat. **105:** 295–324.

SCHOEN, D. J., and R. G. LATTA, 1989 Spatial autocorrelation of genotypes in populations of *Impatiens pallida* and *Impatiens capensis*. Heredity **63:** 181–189.

SOKAL, R. R., 1979 Ecological parameters inferred from spatial correlograms, pp. 167–196 in *Contemporary Quantitative Ecology and Related Econometrics*, edited by G. P. PATIL and M. L. ROSENZWEIG. International Cooperative Publishing House, Fairland, Md.

Sokal, R. R., G. M. Jacquez and M. C. WOOTEN, 1989 Spatial autocorrelation analysis of migration and selection. Genetics **121:** 845–855.

SOKAL, R. R., and P. MENOZZI, 1982 Spatial autocorrelations of HLA frequencies in Europe support demic diffusion of early farmers. Am. Nat. **119:** 1–17.

SOKAL, R. R., and N. L. ODEN, 1978a Spatial autocorrelation in biology. 1. Methodology. Biol. J. Linn. Soc. **10:** 199–228.

SOKAL, R. R., and N. L. ODEN, 1978b Spatial autocorrelation in biology. 2. Some biological implications and four applications of evolutionary and ecological interest. Biol. J. Linn. Soc. **10:** 229–249.

SOKAL, R. R., N. L. ODEN and J. S. F. BARKER, 1987 Spatial structure in *Drosophila buzzatii* populations: simple and directional spatial autocorrelation. Am. Nat. **129:** 122–142.

SOKAL, R. R., P. E. SMOUSE and J. V. NEEL, 1986 The genetic structure of a tribal population, the Yanomama Indians. XV. Patterns inferred by autocorrelation analysis. Genetics **114:** 259–287.

SOKAL, R. R., and D. E. WARTENBERG, 1983 A test of spatial autocorrelation analysis using an isolation-by-distance model. Genetics **105:** 219–237.

SOKAL, R. R., and E. M. WINKLER, 1987 Spatial variation among Kenyan tribes and subtribes. Hum. Biol. **59:** 147–164.

TURNER, M. E., J. C. STEPHENS and W. W. ANDERSON, 1982 Homozygosity and patch structure in plant populations as a result of nearest-neighbor pollination. Proc. Natl. Acad. Sci. USA **79:** 203–207.

WAGNER, D. B., Z.-X. SUN, D. R. GOVINDARAJU and B. P. DANCIK, 1988 The population genetic structure of chloroplast DNA polymorphism in a *Pinus banksiana-P. contorta* sympatric region: spatial autocorrelation, pp. 19–32 in *Molecular Genetics of Forest Trees* (Proceedings of the Frans Kempe Symposium), edited by J. E. HÄLLGREN. Swedish University of Agricultural Science, Umeå, Rep. 8.

WRIGHT, S., 1943 Isolation by distance. Genetics **28:** 114–138.

WRIGHT, S., 1946 Isolation by distance under diverse systems of mating. Genetics **31:** 39–59.

WRIGHT, S., 1965 The interpretation of population structure by *F*-statistics with special regard to systems of mating. Evolution **19:** 395–420.

Communicating editor: B. S. WEIR